Sensors and Actuators A 252 (2016) 96–103

Contents lists available at ScienceDirect

Sensors and Actuators A: Physical

journal homepage: www.elsevier.com/locate/sna

Chlorobenzene sensor based on Pt-decorated porous single-crystalline ZnO nanosheets

Cuiping Gu[a], Huanhuan Huang[a,b], Jiarui Huang[a], Zhen Jin[b], Hanxiong Zheng[b,c], Ning Liu[c], Minqiang Li[b], Jinhuai Liu[b], Fanli Meng[b,*]

[a] College of Chemistry and Materials Science, Center for Nano Science and Technology, Anhui Normal University, Wuhu 241000, China
[b] Nanomaterials and Environment Detection Laboratory, Institute of Intelligent Machines, Chinese Academy of Sciences, Hefei 230031, China
[c] Department of Mechanical and Automotive Engineering, Anhui Polytechnic University, Wuhu 241000, China

ARTICLE INFO

Article history:
Received 9 June 2016
Received in revised form 25 October 2016
Accepted 2 November 2016
Available online 4 November 2016

Keywords:
Chlorobenzene
Sensor
Pt
Porous single-crystalline
ZnO nanosheet

ABSTRACT

Detection of chlorobenzene is a challenge for metal oxide gas sensors because of its stable molecule structure. In this work, Pt-decorated porous single-crystalline ZnO nanosheets (PSC ZnO NSs) were successfully synthesized via a one-pot hydrothermal method followed by a liquid phase reduction process. The morphology and structure of the as-prepared sample were well characterized by X-ray diffraction (XRD), field-emission scanning electron microscopy (FE-SEM), transmission electron microscopy (TEM), energy dispersive spectrum (EDS) and ICP-MS analysis. From gas-sensing test, it can be found that the decoration of Pt nanoparticles largely enhanced the sensing performance of the PSC ZnO NSs. The Pt-decorated PSC ZnO NSs showed good response to low concentrations of chlorobenzene from 10 to 500 ppb. In contrast, the Au and Ag-decorated PSC ZnO NSs had still no response to 500 ppb of chlorobenzene. The enhancement sensing mechanism of Pt nanoparticle decoration has also been discussed in detail.

1. Introduction

Chlorobenzene is a kind of toxic chemical, which has been widely used as a raw material, intermediate and solvent in chemical, agrochemical and pharmaceutical industries [1]. The existence in the environment will largely threaten human health because of its high toxicity and long-term persistence [2]. Therefore, effective detection of chlorobenzene is necessary for strengthening environmental regulations and treatments.

Gas chromatography is currently a widely used method to detect chlorobenzene because of its extremely versatile, sensitive and selective. However, the complicated, time-consumed operation, and expensive cost largely restrict its application in field test. Online process monitoring or low-cost alternative technologies are all important for the determination of chlorobenzene. As we know, the application of metal oxide gas sensors has triggered much attention because of their low cost, easy production, compact size and simple measuring electronics [3,4]. There have been significant advances in the field of metal oxide gas sensors to detect chlorobenzene. For example, Tang et al. reported a chlorobenzene sensor with good sensing properties using single crystalline In_2O_3 nanorods as the active material [5]. Jing et al. fabricated a novel gas sensor based on porous ZnO nanoplates which exhibited good sensing properties to chlorobenzene at low operating temperatures [6]. However, a critical problem is that the metal oxide gas sensors usually show poor response and selectivity towards chlorobenzene because of its stable molecule structure.

As an n-type semiconducting oxide, zinc oxide (ZnO) is considered to be one of the most popular sensing materials because of its large excitation energy, excellent electronic and photonic properties [7–9]. Many efforts have been devoted to obtain high sensing performance for ZnO sensing materials. In the past decade, ZnO nanomaterials with various morphologies have been synthesized, such as nanowires [10], nanotubes [11], nanobelts [12], microspheres [13], hierarchical nanostructures [14], etc. because the morphology and structure can largely affect the performances of the sensing materials [15–19]. Among those nanostructures, porous ZnO nanomaterials were proved with better sensing performance because of the larger surface area and more active sites [20]. Zhang et al. found that the porous ZnO nanosheets show superior sensing response to ethanol, with the detection limit of as low as 10 ppb [21]. Thus, rational design the structure of the ZnO nanomaterial can largely enhance its sensing property.

* Corresponding author.
E-mail address: flmeng@iim.ac.cn (F. Meng).

http://dx.doi.org/10.1016/j.sna.2016.11.004
0924-4247/

Noble metal modification is another effective method to improve the sensing performance. It is known that noble metal nanoparticles, such as Au [22], Ag [23] and Pt [24] nanoparticles, are high-effective oxidation catalysts. Therefore, the modified noble metal nanoparticles would greatly improve the response and selective properties of the ZnO materials for their exceptional catalytic activities. Wang et al. found that the sensing performance of the 3D hierarchically porous ZnO structures increase more than 3 times by Au modification [25]. We also found that the Ag-decorated porous ZnO nanosheets exhibit dramatically sensing performance in ethanol detection and the lowest detection concentration was 1 ppb [26]. The Au-modified hierarchical ZnO structures could detect acetone with the lowest detection concentration of 0.5 ppb [27].

However, the Ag and Au modification showed little response to chlorobenzene, here. Therefore, Pt nanoparticles were decorated on the surfaces of porous single-crystalline ZnO nanosheets (PSC ZnO NSs) through a liquid phase reducing method. Because of the excellent catalytic performace of Pt nanoparticles, the obtained Pt-decorated PSC ZnO NSs exhibit excellent sensing response and selectivity towards chlorobenzene. The detection limit was down to 10 ppb.

2. Experimental

2.1. Materials and materials characterization

All reagents were commercially available from Sinopharm Chemical Reagent Co., Ltd. (China) with analytical grade and were used without further purification.

The morphologies were characterized by field-emission scanning electron microscopy (FE-SEM, FEI Sirion-200) and transmission electron microscopy (TEM, JEOL JEM-2010). Moreover, the crystal structure of the as-prepared samples was determined by X-ray diffraction (XRD, Philips X'pert PRO) with Cu K radiation. Energy dispersive spectroscopy (EDS) was measured by Oxford INCA X-Max 50. Inductively coupled plasma mass spectrometry (ICP-MS) was measured by Thermofisher Scientific iCAP Qc.

2.2. Preparation of the Pt-decorated PSC ZnO NSs

The PSC ZnO NSs were synthesized by a one-pot hydrothermal method followed by an annealing treatment [28]. For loading Pt nanoparticles by a liquid phase reducing method, the preprepared PSC ZnO NSs (20 mg) and 250 μL of sodium chloroplatinate solution (Na_2PtCl_6, 2 wt%) were first dispersed in 10 mL of deionized water in a glass vessel. The mixture solution was stirred for 30 min in ice bath. And then, desired amount of 0.01 M $NaBH_4$ solution were dropwisely added into the mixture solution. Four samples (Pt-ZnO-1, Pt-ZnO-2, Pt-ZnO-3 and Pt-ZnO-4) were prepared by adding different amount of $NaBH_4$ solutions, i.e. 10 μL, 300 μL 500 μL and 1000 μL, respectively. When the color of the solution turns to gray, the Pt-decorated PSC ZnO NSs were obtained. The precipitate was collected by centrifugation, then cleaned with deionized water and ethanol several times, and dried at 60 °C in a vacuum oven. At last the resulting powder was annealed at 300 °C in air for 2 h.

2.3. Fabrication of the gas sensor and the gas sensing measurement system

The as-prepared sensing films were applied for the measurement of gas sensing properties following the fabrication process of the gas sensor as shown in Fig. 1. The structure of the sensor is shown in Fig. 1a. The sensing materials were dispersed in ethanol and then coated onto the ceramic tube of the sensor. After annealing at 300 °C in air for 1 h, the sensing materials were combined with the ceramic tube and the gas sensors were obtained.

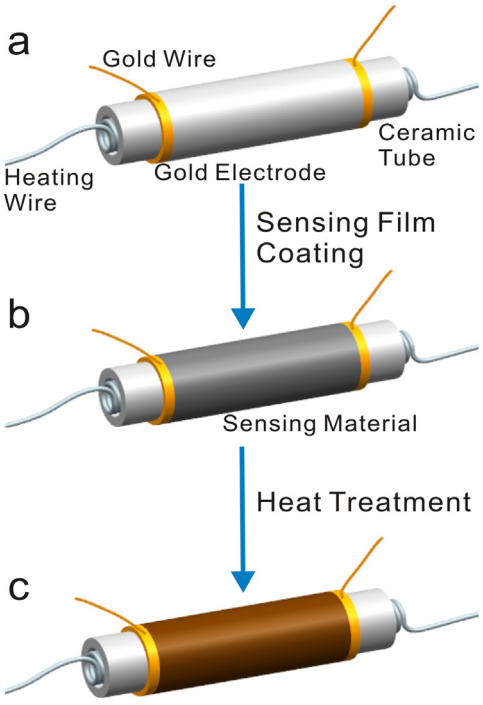

Fig. 1. Schematic diagram of the fabrication process of the gas sensor.

The illustration of the measurement system was shown in our previous work [29]. Briefly, the gas sensing tests were performed using a Keithley 6487 Source/Measure Unit (SMU) measurement system in a closed test chamber with a volume of about 1000 mL equipped with appropriate an inlet and an outlet for gas flow. The gas sensing properties were evaluated at various operation temperatures from 100 to 400 °C by measuring the changes of resistance of the sensor in air. The target gases were prepared by drawing out the headspace vapor into a microsyringe at room temperature. The response of the sensor is defined as:

$$\text{Response} = \frac{R_a}{R_g} = \frac{I_g}{I_a} \quad (1)$$

Here, R_a and R_g are the electric resistance of the sensor in the air and target gas, respectively. I_a and I_g are the electric currents of the sensor in the air and target gas, respectively. The response time is defined as the time when the change of current reaches 90% of the balanced current on exposure to a target gas. Similarly, the recovery time is defined as the time reached a 90% reversal of the current.

3. Results and discussion

3.1. Characterization of the Pt-decorated PSC ZnO NSs

The crystal structures of the un-decorated and the Pt-decorated PSC ZnO NSs were characterized by XRD, and the corresponding diffraction patterns were shown in Fig. 2. For PSC ZnO NSs, all of the diffraction peaks of the pure ZnO can be indexed to wurtzite ZnO (JCPDS 36-1451) [28]. However, after Pt decoration, an additional weak peak at 40.5° can be observed, which is corresponding to the Pt (111) plane.

Fig. 3a and b present the SEM and TEM image of the PSC ZnO NSs, respectively. It can be seen that the nanosheet is quite thin, and full of nanoholes with the size of tens nanometers. The inset in Fig. 3b is the SAED pattern of the PSC ZnO NSs, the well-ordered diffraction dots indicating the single crystalline structure of nanosheets. The

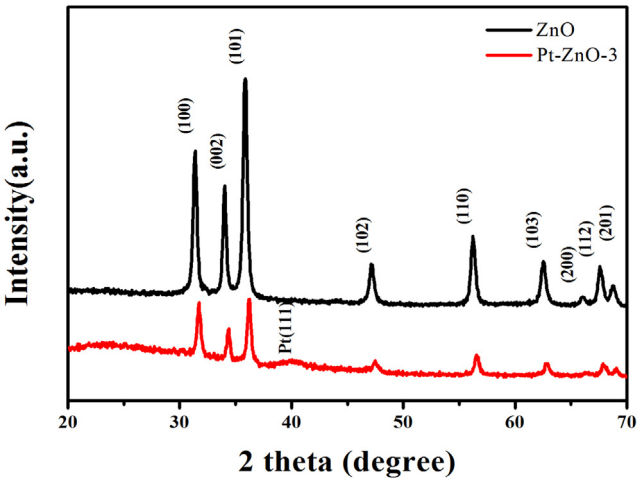

Fig. 2. XRD patterns of the un-decorated and the Pt-decorated PSC ZnO NSs.

Fig. 3c presents the TEM image of the Pt-decorated PSC ZnO NSs. It can be clearly seen that the Pt NPs are uniformly distributed on the PSC ZnO NSs. Fig. 3d is the EDS spectrum from which a obvious Pt peak can be observed, indicating the modification of the Pt nanoparticle on PSC ZnO NSs. The amount of Pt is calculated to be 8.96 wt%.

As a high performance sensing material, the decoration amount of Pt nanoparticles can largely affect its sensing property. Thus, the precise control of the modification amount of Pt nanoparticles was done by adjusting the amount of $NaBH_4$ solution. When the amount of $NaBH_4$ solution is 10 μL (Pt-ZnO-1), it can be seen from Fig. 4a that the Pt nanoparticles were sporadically distributed on the surface of the PSC ZnO NSs. When the amount of $NaBH_4$ solution is 300 μL (Pt-ZnO-2), as shown in Fig. 4b, more Pt nanoparticles can be easily observed. As the amount increased to 500 μL (Pt-ZnO-3), the loading amount of the Pt nanoparticles clearly increased. And the size of the Pt nanoparticles became larger, and the density also further increased (Fig. 4c). When the amount of $NaBH_4$ solution increased to 1000 μL (Pt-ZnO-4), it can be seen that the nanoparticles becomes greatly larger (Fig. 4d), which may be caused by Ostwald ripening. According to the ICP-MS analysis, the decoration amount of Pt nanoparticles is 0.93 wt%, 5.89 wt%, 8.82 wt%, 13.63 wt%, respectively, which is also agreement with the analysis of EDS spectrum.

3.2. Formation process of the Pt-decorated PSC ZnO NSs

In order to obtain the Pt-decorated PSC ZnO NSs, the ZnO nanosheets were firstly dispersed into the Na_2PtCl_6 solution.

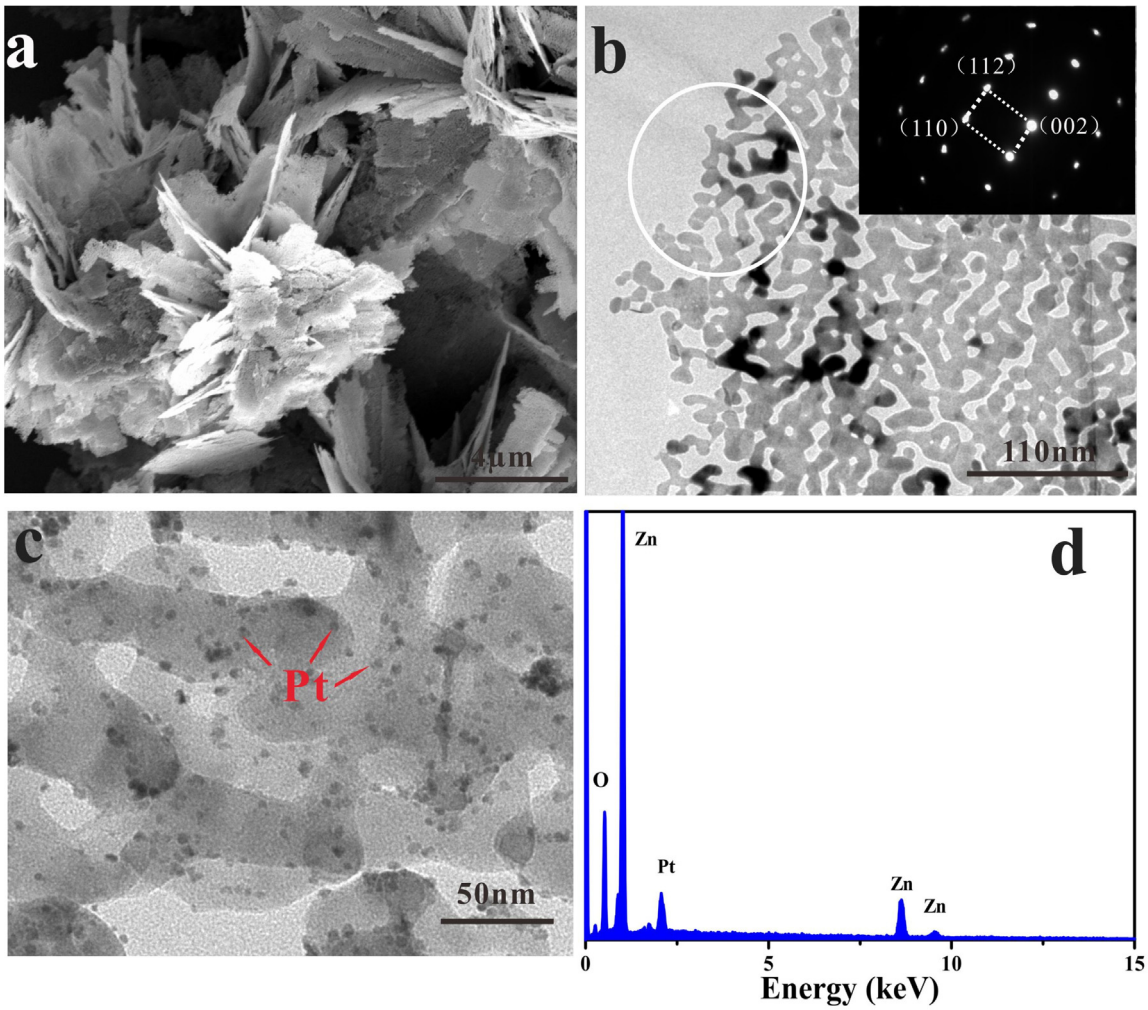

Fig. 3. (a) SEM and (b) TEM images of the PSC ZnO NSs inserted with corresponding SAED pattern in the white circle area. (c) TEM image and (d) EDS spectrum of the Pt decorated PSC ZnO NSs (Pt-ZnO-3).

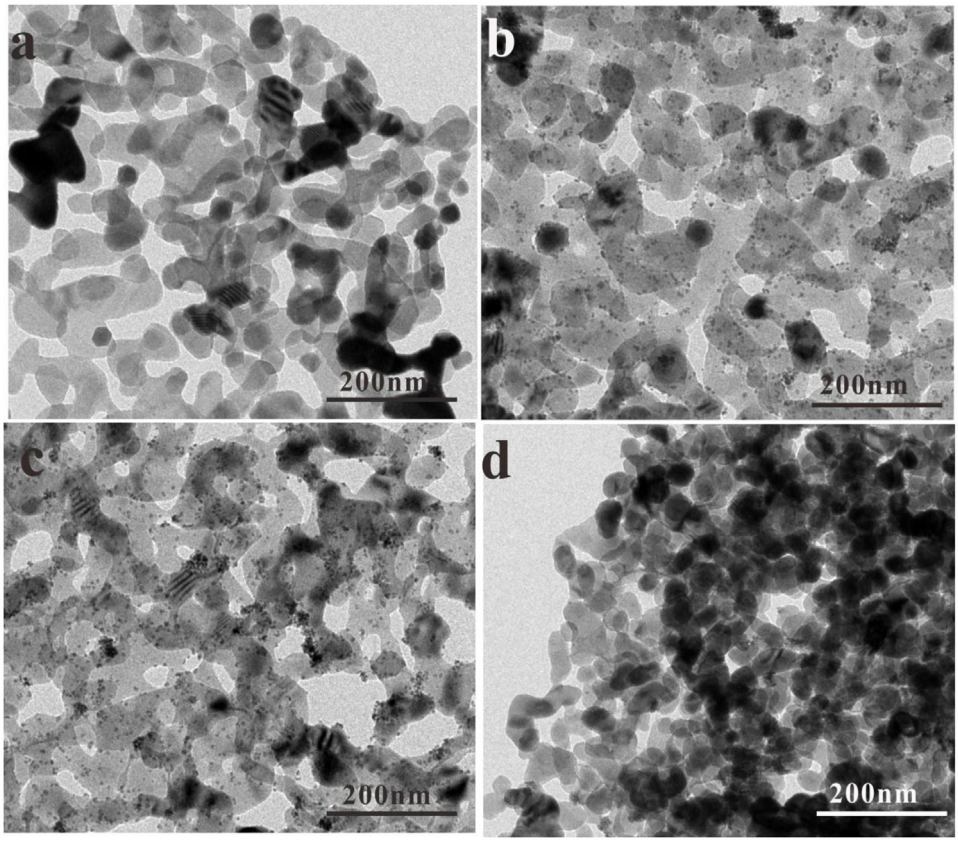

Fig. 4. TEM images of the samples: (a) Pt-ZnO-1, (b) Pt-ZnO-2, (c) Pt-ZnO-3 and (d) Pt-ZnO-4.

Because of the porous structure and large surface area, certain amount of $PtCl_6^{2-}$ ions would adsorbed on the surface of PSC ZnO NSs. As well known, $NaBH_4$ is a strong reducing agent. Thus, when $NaBH_4$ added into the Na_2PtCl_6 solution, the adsorbed $PtCl_6^{2-}$ ions would be reduced as follow process:

$$2PtCl_6^{2-} + BH_4^- + 4H_2O \rightarrow 2Pt + B(OH)_4^- + 8H^+ + 12Cl^- \quad (2)$$

In this way, Pt nanoparticles would form on the surface of the PSC ZnO NSs. When the amount of $NaBH_4$ increased, more $PtCl_6^{2-}$ can be reduced, and consequently, the Pt nanoparticles could act as the nucleation center and grown up. However, when the amount of $NaBH_4$ continues increased, the size of Pt nanoparticles would keep growing and several closed nanoparticles would merge together to form a larger nanoparticle. This would be the reason why the Pt nanoparticles aggregated when the added amount of $NaBH_4$ reaches to 500 μL.

3.3. Operating temperature of the Pt-decorated PSC ZnO NSs based sensor

Operating temperature is very important for the sensing performance of metal oxide gas sensors. Therefore, we systematically investigated that the responses of the Pt-decorated PSC ZnO NSs to 500 ppb of chlorobenzene at different operating temperatures as shown in Fig. 5. It can be seen that the responses increase firstly and then present a turning point at 300 °C with increasing operating temperature, indicating the optimal operating temperature was 300 °C. Thus, the following tests were carried out at 300 °C. According to Wolkenstein's model for semiconductors [30], the surface reactions of the target gases is usually highly dependent on the activity of the adsorbed oxygen species. Generally speaking, the molecular (O_2^-) form works mostly below 150 °C, while the atomic species (O^-,O^{2-}) play a dominant role at the temperature higher than 150 °C [31]. In our cases, the optimal operating temperature of 300 °C suggests that the atomic species mostly dominates the gas sensor, which is more active for reaction with target gas. However, desorption will dominate the adsorption balance between the sensing material and the target gas when the temperature increase higher. Therefore, there is an optimal operating temperature.

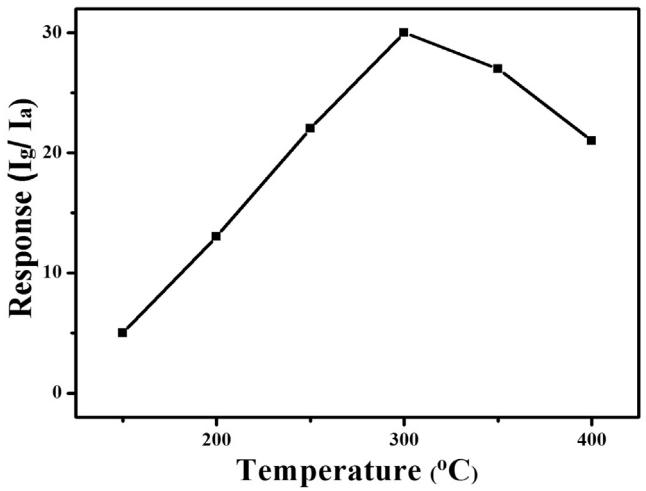

Fig. 5. Responses of the Pt-ZnO-3 to 500 ppb of chlorobenzene at different operating temperatures.

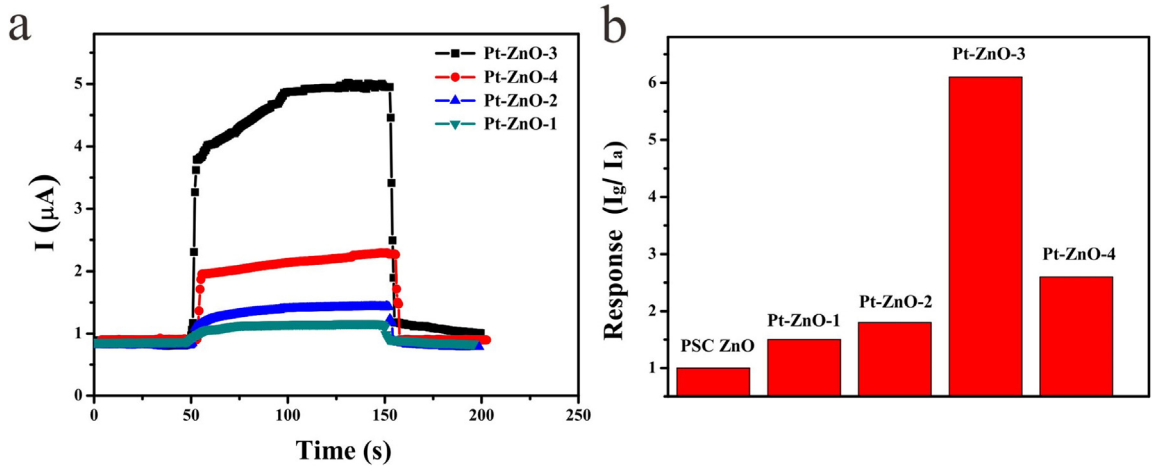

Fig. 6. (a) Real-time responses and (b) responses of Pt-decorated PSC ZnO NSs with different Pt contents to 30 ppb of chlorobenzene at 300 °C.

3.4. Gas sensing properties of the Pt-decorated PSC ZnO NSs based sensor

The sensing properties of the PSC ZnO NSs with different Pt decorated amount were analyzed. Fig. 6a shows that the real-time responses of the Pt-decorated PSC ZnO NSs with different Pt loading amount to 30 ppb of chlorobenzene at 300 °C. It can be seen that the response of the Pt-decorated PSC ZnO NSs (Pt-ZnO) gradually increased as the decoration amount of the Pt nanoparticles increased from Pt-ZnO-1 to Pt-ZnO-3. However, when the decoration amount of the Pt nanoparticles continuously increased to Pt-ZnO-4, the responses of the sample decreased. Fig. 6b summarized the responses of the Pt-decorated PSC ZnO NSs based sensors with different Pt decoration amount. It can be seen that the un-decorated PSC ZnO showed no response to 30 ppb of chlorobenzene. When the decoration amounts of Pt nanoparticles are different on the surfaces of Pt-ZnO-1, Pt-ZnO-2, Pt-ZnO-3, Pt-ZnO-4, the responses towards chlorobenzene are 1.5, 1.8, 6.1 and 2.6, respectively. Obviously, it can be seen that the Pt-ZnO-3 possess the highest performance. Pt-ZnO-3 also shows the shortest response and recovery times among the four samples, which are 20 s and 10 s, respectively. In the same way, the response and recovery times are 25 s and 26 s for Pt-ZnO-1, 41 s and 16 s for Pt-ZnO-2, 43 s and 16 s for Pt-ZnO-4, respectively. The sensing performance of the Pt-ZnO-4 decreases because the Pt nanoparticles grew larger by Ostwald ripening as shown in Fig. 4d, which makes the exposed Pt atoms decrease.

The gas sensing properties of the Pt-ZnO-3 to different concentrations of chlorobenzene have also been investigated as shown in Fig. 7. It is obviously observed that the responses of the Pt-decorated PSC ZnO NSs increased as the concentration increased from 10 to 500 ppb. It can also be observed from the response curves that the Pt-decorated PSC ZnO NSs possess low electric noise and high signal-to-noise ratio (S/N), which can be attributed to the single-crystalline structure of the ZnO nanosheets. Fig. 8 summarized the corresponding plots of the response vs concentration of the Pt-decorated PSC ZnO NSs. In order to further illustrate the effect of the decorated noble metals, the responses of the pure PSC ZnO NSs, Au-decorated PSC ZnO NSs (Au-ZnO), and Ag-decorated PSC ZnO NSs (Ag-ZnO) towards chlorobenzene were also present, which were reported in our previous works [26,27]. It can be seen that, the approximately linear relationships between response and gas concentration suggest that the Pt decorated ZnO NSs exhibits a good sensing performance to chlorobenzene. However, the pure

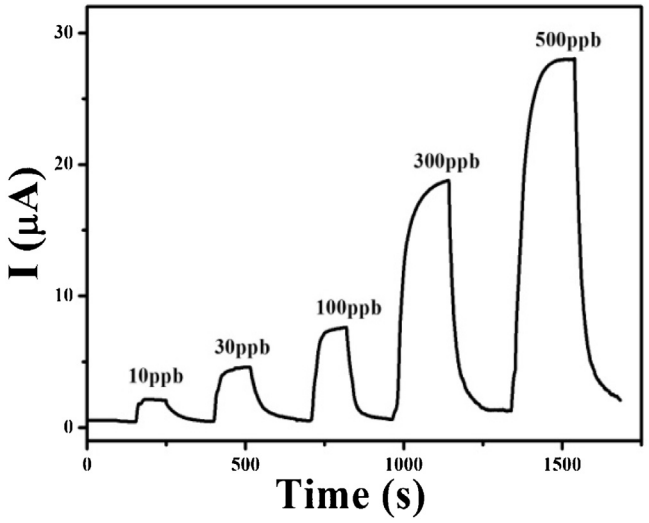

Fig. 7. Real-time responses of the Pt-ZnO-3 to different concentrations of chlorobenzene at 300 °C.

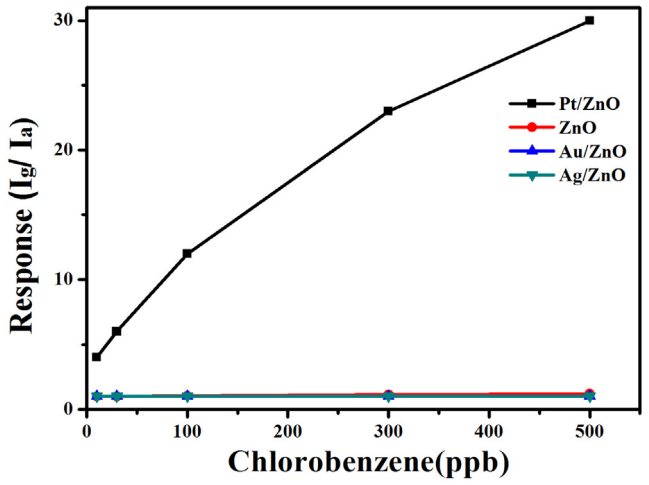

Fig. 8. Responses of the un-decorated and different noble metal-decorated PSC ZnO NCs to chlorobenzene at 300 °C.

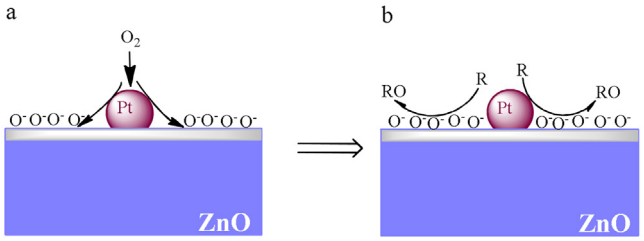

Fig. 9. Sensing mechanism of the Pt-decorated PSC ZnO NCs (a) before and (b) after target gas is introduced.

PSC ZnO NSs only have a small responsive sensitivity of 1.2–500 ppb chlorobenzene, while, the Au and Ag-decorated PSC ZnO NSs have no response to 500 ppb chlorobenzene. The obvious enhancement of Pt-decorated ZnO NSs in response to chlorobenzene may due to the great catalytic activity of Pt particles [32].

3.5. Sensing mechanism of the Pt-decorated PSC ZnO NSs based sensor

The sensing mechanism of the Pt-decorated PSC ZnO NCs is shown in Fig. 9. Noble metals such as Pt, Au and Ag usually act as electron traps to enhance the charge separation at the interface between the metal particles and ZnO. Generally, the sensing mechanism of noble metal-decoration is to enhance catalytic activity and adjust electrical resistance of the intrinsic metal oxide [33]. It is accordingly considered that the enhanced sensing performance of noble metal-decorated sensors originates from a combination of electronic sensitization mechanisms and chemical sensitization mechanisms [34]. The electronic sensitization caused by interfacial electronic redistribution and the chemical sensitization caused by interfacial atom transport. For Pt nanoparticle-decorated ZnO, the oxygen molecules react preferentially with the Pt nanoparticle forming oxygen anions in air and then spill over to the ZnO matrix. There may be two reaction paths for sensing process. When the target gases are adsorbed on to the surface of the Pt nanoparticle, they are activated by Pt nanoparticle and then migrate to the oxide surface to react with surface oxygen species thereby increasing the surface conductivity (chemical sensitization). Another path is to react with surface oxygen species directly to increase the surface conductivity (electronic sensitization). The electronic and chemical sensitization effects of Pt nanoparticles are pronounced in the sensing of Pt-ZnO to chlorobenzene, thereby resulting in its enhanced performance, compared to bare ZnO. In contrast, the chemical sensitization effects are weak for Au or Ag nanoparticles [35], which may cause that the sensing properties of Au-ZnO and Ag-ZnO showed worse to Pt-ZnO.

3.6. Stability and selectivity of the Pt-decorated PSC ZnO NSs based sensor

The stability of the sensor device is a very important parameter for practical applications. Thus, the reproducibility of the Pt-decorated PSC ZnO NS based sensor has been investigated by the response curves of the Pt-decorated PSC ZnO NSs to 300 ppb of chlorobenzene after 5 cycles. From Fig. 10, it can be seen that the Pt-decorated PSC ZnO NSs exhibits rather good stability and repeatability, and the maximum deviation was an acceptable range ensuring relatively high stability. Because of their high sensitivity, rapid response, and good repeatability, the Pt-decorated PSC ZnO NSs based gas sensors have promising industrial applications.

Selectivity is another key parameter for gas sensor. High selectivity of the gas sensors is beneficial for application. ZnO nanostructure based sensors were reported to show responses to many

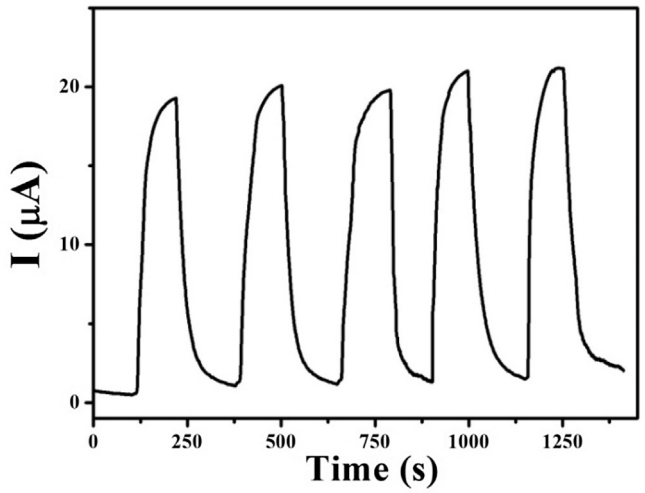

Fig. 10. Response curves of the Pt-ZnO-3 to 300 ppb chlorobenzene after 5 cycles of gas on and off at 300 °C.

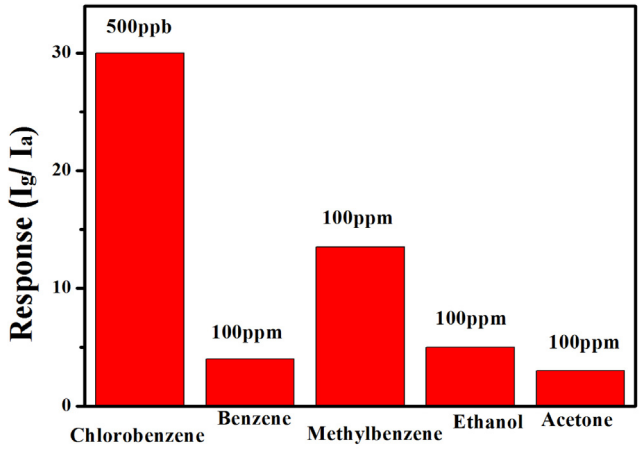

Fig. 11. Response of the Pt-ZnO-3 to 500 ppb of chlorobenzene and 100 ppm of other VOCs at 300 °C.

gases, including ethanol, benzene, toluene, etc. [36]. However, in our case, as shown in Fig. 11, it can be found that the response of the Pt decorated PSC ZnO NSs to 500 ppb of chlorobenzene is much higher than that to 100 ppm of other VOC gases. This result indicated that the Pt decorated PSC ZnO NSs exhibit excellent selectivity to chlorobenzene. It is believed that the Pt-decorated PSC ZnO NSs will enable us to provide a new pathway for designing novel trace chlorobenzene sensors.

4. Conclusions

In summary, Pt-decorated PSC ZnO NSs were synthesized through a one-pot hydrothermal method followed by a liquid phase reducing method. The vapors of chlorobenzene have been detected by the Pt-decorated PSC ZnO NSs sensors. Because of the excellent catalytic activity of Pt particles, the Pt-decorated PSC ZnO NSs showed distinctly greater response. The influence of the Pt decorated amount was also studied. We found that when the amount of $NaBH_4$ (0.01 M) is 500 μL, it showed best sensing performance towards chlorobenzene, and the detection limit reaches 10 ppb. What's more, the Pt-decorated PSC ZnO NSs exhibit good sensing selectivity towards chlorobenzene, indicating its potential application as a novel trace chlorobenzene sensor.

Acknowledgements

We appreciate the financial support of the National Basic Research Program of China (2013CB934304), the National Natural Science Foundation of China (61374017, 61573334 and 31571567) and the Key Technologies R & D Program of Anhui Province (1501021005).

References

[1] I.M. Nangoi, P.K. Kiyohara, L.M. Rossi, Catalytic hydrodechlorination of chlorobenzene over supported palladium catalyst in buffered medium, Appl. Catal. B 100 (2010) 42–46.
[2] A. Aznarez, R. Delaigle, P. Eloy, E.M. Gaigneaux, S.A. Korili, A. Gil, Catalysts based on pillared clays for the oxidation of chlorobenzene, Catal. Today 246 (2015) 15–27.
[3] N. Vorobyeva, M. Rumyantseva, D. Filatova, E. Konstantinova, D. Grishina, A. Abakumov, S. Turner, A. Gaskov, Nanocrystalline ZnO(Ga): paramagnetic centers, surface acidity and gas sensor properties, Sens. Actuators B 182 (2013) 555–564.
[4] D.D. Li, J. Hu, R.Q. Wu, J.G. Lu, Conductometric chemical sensor based on individual CuO nanowires, Nanotechnology 21 (2010) 485502.
[5] Y.J. Tang, J.M. Ma, In_2O_3 nanostructures: synthesis and chlorobenzene sensing properties, RSC Adv. 4 (2014) 25692–25697.
[6] Z.H. Jing, J.H. Zhan, Fabrication and gas-sensing properties of porous ZnO nanoplates, Adv. Mater. 20 (2008) 4547–4551.
[7] S.R. Ryu, S.D.G. Ram, H.D. Cho, D.J. Lee, T.W. Kang, Y. Woo, Single ZnO nanocactus gas sensor formed by etching of ZnO nanorod, Nanoscale 7 (2015) 11115–11122.
[8] M. Chen, Z.H. Wang, D.M. Han, F.B. Gu, G.S. Guo, Porous ZnO polygonal nanoflakes: synthesis, Uue in high-sensitivity NO_2 gas sensor, and proposed mechanism of gas sensing, J. Phys. Chem. C 115 (2011) 12763–12773.
[9] C.P. Gu, J.R. Huang, Y.J. Wu, M.H. Zhai, Y.F. Sun, J.H. Liu, Preparation of porous flower-like ZnO nanostructures and their gas-sensing property, J. Alloys Compd. 509 (2011) 4499–4504.
[10] C. Gu, S. Li, J. Huang, C. Shi, J. Liu, Preferential growth of long ZnO nanowires and its application in gas sensor, Sens. Actuators B 177 (2013) 453–459.
[11] Y. Qiu, H. Zhang, L. Hu, D. Yang, L. Wang, B. Wang, J. Ji, G. Liu, X. Liu, J. Lin, F. Li, S. Han, Flexible piezoelectric nanogenerators based on ZnO nanorods grown on common paper substrates, Nanoscale 4 (2012) 6568–6573.
[12] X.D. Wang, Y. Ding, C.J. Summers, Z.L. Wang, Large-scale synthesis of six-nanometer-wide ZnO nanobelts, J. Phys. Chem. B 108 (2004) 8773–8777.
[13] N. Tripathy, R. Ahmad, H.S. Jeong, Y.B. Hahn, Time-dependent control of hole-opening degree of porous ZnO hollow microspheres, Inorg. Chem. 51 (2012) 1104–1110.
[14] H.J. Zhang, R.F. Wu, Z.W. Chen, G. Liu, Z.N. Zhang, Z. Jiao, Self-assembly fabrication of 3D flower-like ZnO hierarchical nanostructures and their gas sensing properties, CrystEngComm 14 (2012) 1775–1782.
[15] Y. Guan, D.W. Wang, X. Zhou, P. Sun, H.Y. Wang, J. Ma, G.Y. Lu, Hydrothermal preparation and gas sensing properties of Zn-doped SnO_2 hierarchical architectures, Sens. Actuators B 191 (2014) 45–52.
[16] H. Wu, C. Xu, J. Xu, L.F. Lu, Z.Y. Fan, X.Y. Chen, Y. Song, D.D. Li, Enhanced supercapacitance in anodic TiO_2 nanotube films by hydrogen plasma treatment, Nanotechnology 24 (2013) 455401.
[17] G.Y. Lu, J. Xu, J.B. Sun, Y.S. Yu, Y.Q. Zhang, F.M. Liu, UV-enhanced room temperature NO_2 sensor using ZnO nanorods modified with SnO_2 nanoparticles, Sens. Actuators B 162 (2012) 82–88.
[18] C. Xu, Y. Song, L.F. Lu, C.W. Cheng, D.F. Liu, X.H. Fang, X.Y. Chen, X.F. Zhu, D.D. Li, Electrochemically hydrogenated TiO_2 nanotubes with improved photoelectrochemical water splitting performance, Nanoscale Res. Lett. 8 (2013) 391.
[19] H. Wu, D.D. Li, X.F. Zhu, C.Y. Yang, D.F. Liu, X.Y. Chen, Y. Song, L.F. Lu, High-performance and renewable supercapacitors based on TiO_2 nanotube array electrodes treated by an electrochemical doping approach, Electrochim. Acta 116 (2014) 129–136.
[20] F.L. Meng, N.N. Hou, S. Ge, B. Sun, Z. Jin, W. Shen, L.T. Kong, Z. Guo, Y.F. Sun, H. Wu, C. Wang, M.Q. Li, Flower-like hierarchical structures consisting of porous single-crystalline ZnO nanosheets and their gas sensing properties to volatile organic compounds (VOCs), J. Alloys Compd. 626 (2015) 124–130.
[21] L.X. Zhang, J.H. Zhao, H.Q. Lu, L. Li, J.F. Zheng, H. Li, Z.P. Zhu, Facile synthesis and ultrahigh ethanol response of hierarchically porous ZnO nanosheets, Sens. Actuators B 161 (2012) 209–215.
[22] X.H. Liu, J. Zhang, X.Z. Guo, S.H. Wu, S.R. Wang, Amino acid-assisted one-pot assembly of Au, Pt nanoparticles onto one-dimensional ZnO microrods, Nanoscale 2 (2010) 1178–1184.
[23] Q. Xiang, G.F. Meng, Y. Zhang, J.Q. Xu, P.C. Xu, Q.Y. Pan, W.J. Yu, Ag nanoparticle embedded-ZnO nanorods synthesized via a photochemical method and its gas-sensing properties, Sens. Actuators B 143 (2010) 635–640.
[24] X.Y. Xue, Z.H. Chen, L.L. Xing, C.H. Ma, Y.J. Chen, T.H. Wang, Enhanced optical and sensing properties of one-step synthesized Pt-ZnO nano flowers, J. Phys. Chem. C 114 (2010) 18607–18611.
[25] X.H. Liu, J. Zhang, L.W. Wang, T.L. Yang, X.Z. Guo, S.H. Wu, S.R. Wang, 3D hierarchically porous ZnO structures and their functionalization by Au nanoparticles for gas sensors, J. Mater. Chem. 21 (2011) 349–356.
[26] F.L. Meng, N.N. Hou, Z. Jin, B. Sun, Z. Guo, L.T. Kong, X.H. Xiao, H. Wu, M.Q. Li, J.H. Liu, Ag-decorated ultra-thin porous single-crystalline ZnO nanosheets prepared by sunlight induced solvent reduction and their highly sensitive detection of ethanol, Sens. Actuators B 209 (2015) 975–982.
[27] F.L. Meng, N.N. Hou, Z. Jin, B. Sun, W.Q. Li, X.H. Xiao, C. Wang, M.Q. Li, J.H. Liu, Sub-ppb detection of acetone using Au-modified flower-like hierarchical ZnO structures, Sens. Actuators B 219 (2015) 209–217.
[28] Z. Jin, Y.X. Zhang, F.L. Meng, Y. Jia, T. Luo, X.Y. Yu, J. Wang, J.H. Liu, X.J. Huang, Facile synthesis of porous single crystalline ZnO nanoplates and their application in photocatalytic reduction of Cr(VI) in the presence of phenol, J. Hazard. Mater. 276 (2014) 400–407.
[29] F.L. Meng, S. Ge, Y. Jia, B. Sun, Y.F. Sun, C. Wang, H. Wu, Z. Jin, M.Q. Li, Interlaced nanoflake-assembled flower-like hierarchical ZnO microspheres prepared by bisolvents and their sensing properties to ethanol, J. Alloys Compd. 632 (2015) 645–650.
[30] H. Haick, M. Ambrico, T. Ligonzo, R.T. Tung, D. Cahen, Controlling semiconductor/metal junction barriers by incomplete, nonideal molecular monolayers, J. Am. Chem. Soc. 128 (2006) 6854–6869.
[31] N. Barsan, U. Weimar, Conduction model of metal oxide gas sensors, J. Electroceram. 7 (2001) 143–167.
[32] B.L. An, Y.H. Fu, F.Z. Dai, J.Q. Xu, Platinum nanoparticle modified TiO_2 nanorods with enhanced catalytic performances, J. Alloys Compd. 622 (2015) 426–431.
[33] Y.F. Sun, S.B. Liu, F.L. Meng, J.Y. Liu, Z. Jin, L.T. Kong, J.H. Liu, Metal oxide nanostructures and their gas sensing properties: a review, Sensors 12 (2012) 2610–2631.
[34] C. Liu, Q. Kuang, Z. Xie, L. Zheng, The effect of noble metal (Au Pd and Pt) nanoparticles on the gas sensing performance of SnO_2-based sensors: a case study on the {221} high-index faceted SnO_2 octahedra, CrystEngComm 17 (2015) 6308.
[35] V. Srivastava, K. Jain, Highly sensitive NH_3 sensor using Pt catalyzed silica coating over WO_3 thick films, Sens. Actuators B 133 (2008) 46–52.
[36] Z. Bai, C. Xie, S. Zhang, L. Zhang, Q. Zhang, W. Xu, J. Xu, Microstructure and gas sensing properties of the ZnO thick film treated by hydrothermal method, Sens. Actuators B 151 (2010) 107–113.

Biographies

Cuiping Gu was born in Xuancheng Anhui Province. She received her B.S. in Chemistry from the College of Chemistry and Materials Science of Anhui Normal University in 2000, her M.S. in Polymer Chemistry from the School of Chemistry and Chemical Engineering of Anhui University in 2005, and her Ph.D. in Inorganic Chemistry from the School of Chemistry and Chemical Engineering of Anhui University in 2008. She is a lecturer of inorganic chemistry at Anhui Normal University. Her present work mainly focuses on sensing materials and biochemistry sensors.

Huanhuan Huang received the B.S. Degree in chemistry from Anhui Normal University, China, in 2014. She is working toward the M.S. degree at Anhui Normal University. Her current research mainly focuses on the nanomaterials and their applications in gas sensors.

Jiarui Huang was born in Shouxian Anhui Province. He received the BS degree in Chemistry from Anhui Normal University, Chemistry Department, in 2000 and the MS degree in synthetic organic chemistry from Nanjing University of technology, Chemistry Department, in 2003 and the PhD degree in Inorganic Chemistry from University of Science and Technology of China, Department of Chemistry, in 2006. He is an Associate Professor of Inorganic Chemistry at Anhui Normal University. Now his work mainly focuses on the sensing materials, gas sensor and biochemistry sensors.

Zhen Jin received the B.S. degree in electronic science and technology from Anhui University, China, in 2003 and the Ph.D. degree in condensed materials from Institute of Solid State Physics, Chinese Academy of Sciences, China, in 2009. Currently, he works as a post doctor at Institute of Intelligent Machines, Chinese Academy of Sciences, China. His current research interests include synthesis of enviromental sensing nanomaterials and fabrication of nanosensors.

Hanxiong Zheng received the B.S. degree in material forming and control engineering from Anhui Polytechnic University, China, in 2014. Since September 2014, he has been a graduate student in Department of Mechanical and Automotive Engineering at Anhui Polytechnic University of China. He is doing his Master's Thesis at Institute of Intelligent Machines, Chinese Academy of Science, China. His current research interests include nanomaterials and their applications in gas sensors.

Ning Liu received his M.S. degree from Anhui Normal University, China, in 1982. Currently, He works in Anhui Polytechnic University, China. His work focuses on the study of synthesis methods of nanomaterials and their applications.

Minqiang Li received the B.S. degree in semiconductor material and device from University of Electronic Science and Technology of China in 1986. Since then, he has been at Institute of Intelligent Machines, Chinese Academy of Sciences, China, and currently as a Researcher. His current research interests include semiconductor sensors, gas nanosensors and their applications in detecting hazardous gases.

Jinhuai Liu received the B.S. degree in inorganic chemistry from Yunnan Agricultural University, China, in 1982 and the Ph.D. degree in inorganic chemistry from Graduate University of Chinese Academy of Sciences, China, in 2003. He is currently a professor in Institute of Intelligent Machines, Chinese Academy of Sciences, China. He had been a Visiting Scholar in the Department of Chemistry at the Brown University, USA, from September 1986 to September 1988 and in the New York University of Technology, USA, from October 1988 to December 1989. As a Visiting Scientist, he had been in University of Cincinnati, USA, from July 1993 to August 1994 and Toyohashi University of Technology, Japan, from March to June 1996, respectively. His current research interests include biomimetric material, gas sensing nanomaterial and nanodevice, sensing technology and their applications in detecting hazardous gases and drug/explosive.

Fanli Meng received the B.S. degree in Chemistry from Nanjing University of Science and Technology, in 2002, and the M.S. degree in Inorganic Chemistry from Institute of Intelligent Machines, Chinese Academy of Sciences, in 2005. He received his Ph.D. degree at University of Science and Technology of China, in 2009. He did research at University of California, Los Angeles as a visiting scholar from Feb. 2013 to Feb. 2014. His current work mainly focuses on the sensing materials and nanosensors. He is currently a member of the editorial board of Journal of Sensors.